Quadrilateral Mesh Generation on Trimmed NURBS Surfaces

Soo-Won Chae*[†]
Department of Mechanical Engineering, Korea University
Ki-Youn Kwon
Graduate Student, Department of Mechanical Engineering, Korea University

An automatic mesh generation scheme with unstructured quadrilateral elements on trimmed NURBS surfaces has been developed. In this paper NURBS surface geometries in the IGES format have been employed to represent geometric models. For unstructured mesh generation with quadrilateral elements, a domain decomposition algorithm employing loop operators has been modified. As for the surface meshing, an indirect 2D approach is proposed in which both quasi-expanded planes and projection planes are employed. Sample meshes for complex models are presented to demonstrate the robustness of the algorithm.

Key Words : Trimmed NURBS Surfaces, Quadrilateral Mesh, Domain Decomposition Algorithm, Loop Operators

1. Introduction

Automation of the modeling process for engineering analysis, especially the automatic mesh generation for finite element analysis, has been an important issue in today's engineering environment. Much research efforts have been focused on the mesh generation, and many reliable softwares are commercially available now. Of particular interest is the mesh generation with quadrilateral elements on three-dimensional NURBS surfaces, which are widely used for the analysis of structures with plates and shells, and of the manufacturing processes such as injection molding, sheet metal forming, etc.

Unstructured quadrilateral mesh generators can be grouped into two main approaches: direct and indirect (Owen, 1998). In direct approaches, a domain decomposition method and an advancing front method have been used most widely. In direct approaches, quadrilateral elements are directly generated individually or in groups. As for the domain decomposition methods, Talbert and Parkinson(1991) have developed the recursive decomposition algorithm for the meshing of arbitrarily shaped domains, and generalized the operators for six-node loop during meshing process. Chae et al. (1993, 1997) have proposed enhancements to this method by introducing eight-node loop operators. Zhu et al. (1991) has first proposed an advancing front method, in which elements are formed by projecting edges towards the interior from the boundary. Blacker and Stephenson(1991) suggested the paving method, which is based on iteratively layering or paving rows of elements to the interior of a region's boundary. White and Kinney(1997) has proposed enhancements to the paving algorithm suggesting individual placement of elements. The direct approach can produce meshes of high quality, but the algorithms are usually complicated and not easy to implement. In indirect approaches, triangular elements are generated first, and through the operation of combining and splitting the triangles, quadrilateral elements are constructed indirectly (Lee et al., 1994; Johnston et al., 1991;

[†] First Author

[*] Corresponding Author,
E-mail : swchae@korea.ac.kr
TEL : +82-2-3290-3367; **FAX** : +82-2-926-9441
Department of Mechanical Engineering, Korea University, 5-1 Anam-dong, Sungbuk-ku, Seoul 136-701, Korea.

(Manuscript **Received** November 27, 2000 ; **Revised** February 15, 2001)

Owen et al., 1998). One advantage of the indirect approach is that it employs the triangulation schemes for which numerous reliable algorithms have been developed so far, but one drawback is that the mesh quality is not usually as good as the ones generated by the direct approach, and thus much research efforts have been focused on the mesh quality improvement. In this paper, we have modified a domain decomposition algorithm employing loop operators, which is based on our previous works (Chae et al., 1993; 1997). The modification is made regarding the determination of the best splitting lines in order to improve the mesh quality in certain cases. As for the quadrilateral elements, both four-node and eight-node elements can be employed for the mesh generation.

Surface meshing algorithms can be grouped as either indirect 2D or direct 3D. In indirect 2D approach, some forms of two dimensional parametric planes are employed for the mesh generation and the constructed meshes are transformed to 3D surfaces. In order to obtain good parametrization of the surfaces the surface derivatives should not vary widely over the domain. Some exact arc-length reparameterizations have been defined (Farouki, 1997), but can be excessively costly. Tristano et al. (1998) has proposed an advancing front surface mesh generation in the parametric space using a Riemannian surface definition. George and Bourouchaki (1998) proposed the use of a metric derived from the first fundamental form of the surface. Lee and Joun (1998) have proposed a remapping plane for mesh generation. In direct 3D approach, meshes are constructed directly on three-dimensional surfaces. Lau et al. (1995, 1996) have presented an advancing front approach for arbitrary 3D surfaces. Cass et al. (1996) have implemented the paving algorithm directly on 3D surfaces. In this method, surface normals and tangents are computed in order to determine the direction of the advancing front, and a large number of surface projections are required to ensure that new nodes remain on the surface. In this paper, we propose an indirect approach using both quasi-expanded planes and projection planes for mesh generation, which are the enhancements to the ones using projection planes (Chae and Jung, 1997) and remapping planes (Lee and Joun, 1998).

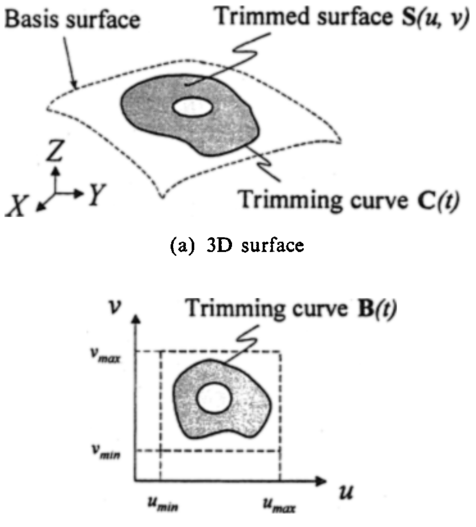

(a) 3D surface

(b) Surface in parametric space

Fig. 1 Trimmed parametric surface

2. Geometry Input for Mesh Generation

Surface models constructed in CAD systems generally have two types of surfaces, analytical and sculptured. Analytical surfaces involve cylindrical, conical, spherical surfaces and surface of revolution, while sculptured surfaces involve blending, Bezier, and NURBS surfaces, etc. However, most of CAD systems provide surface information as NURBS surfaces in order to exchange data with different systems. In this paper trimmed NURBS surfaces in the IGES format are employed for generality in the geometry input.

2.1 Trimmed NURBS surfaces

In CAD systems, trimmed surfaces and basis surfaces are represented by trimmed parametric surfaces, and the boundary curves of trimmed surfaces are called the trimming curves. As shown in Fig. 1, mappings between parametric domains and 3D surfaces are represented by surface equations S(u, v), and the trimming curves

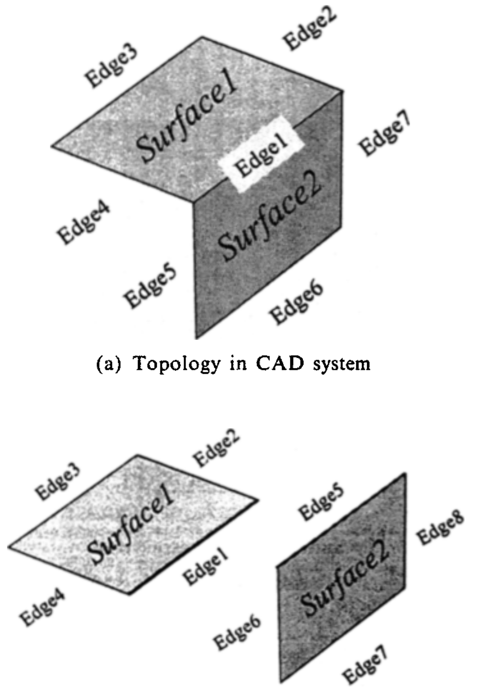

(a) Topology in CAD system

(b) Topology in IGES file

Fig. 2 Characteristics of the IGES format

defined by B(t) in parametric domains are represented by C(t) given in Eq. (1).

$$\begin{aligned}
&S(u, v)=(X(u, v), Y(u, v), Z(u, v)) \\
&(u_{\min}\leq u\leq u_{\max}, v_{\min}\leq v\leq v_{\max}) \\
&B(t)=(u(t), v(t)) \ (t_{\min}\leq t\leq t_{\max}) \\
&C(t)=S(B(t))=S(u(t), v(t)) \\
&\quad =(X(u(t), v(t)), Y(u(t), v(t)), Z \\
&\quad (u(t), v(t))) \qquad (1)
\end{aligned}$$

In this paper NURBS surfaces are employed for representing trimmed surfaces and basis surfaces. The NURBS surface S(u, v), with order p in the u-parametric direction and order q in the v-parametric direction, is defined as follows.

$$S(u, v)=\frac{\sum_{i=0}^{n}\sum_{j=0}^{m}N_{i,p}(u)N_{j,q}(v)w_{i,j}P_{i,j}}{\sum_{i=0}^{n}\sum_{j=0}^{m}N_{i,p}(u)N_{j,q}(v)w_{i,j}} \qquad (2)$$

$$u_{\min}\leq u\leq u_{\max}, \ v_{\min}\leq v\leq v_{\max}$$

where

$S(u, v)$: point on surface
$N_{i,p}(u)$: ith B-splinebasis fuction
$N_{j,q}(v)$: jth B-spline basis fuction

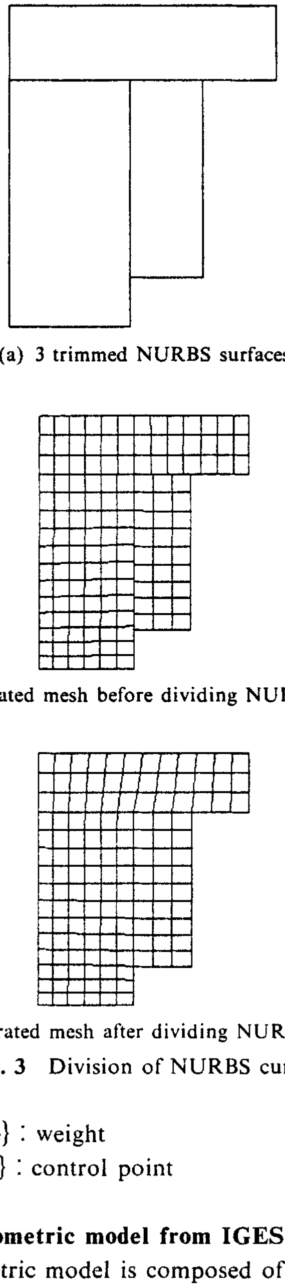

(a) 3 trimmed NURBS surfaces

(b) Generated mesh before dividing NURBS curves

(c) Generated mesh after dividing NURBS curves

Fig. 3 Division of NURBS curves

$\{w_{i,j}\}$: weight
$\{P_{i,j}\}$: control point

2.2 Geometric model from IGES file

A geometric model is composed of the geometry of each component and the topology on the connectivity between entities. In this paper, geometry information is obtained from IGES entity No. 126 and No. 128, which are the rational B-spline curve and rational B-spline surface, respectively, while topology information is obtained from IGES entity No. 102, No. 142 and No. 144, which are composite curve, curve on a parametric surface, and trimmed parametric sur-

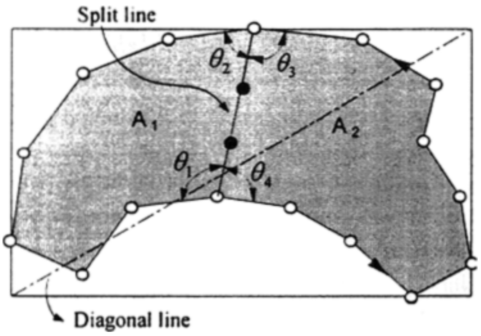

Fig. 4 An example of a candidate split line

face, respectively. As shown in Fig. 2, the IGES format transfers geometric data by separated surfaces, and thus further processing is necessary to obtain a complete model for mesh generation. Since meshes are generated on each surface separately, the nodes generated on the common boundaries may not coincide with each other, which are not valid models for finite element analysis. Therefore, in this paper, common boundaries between adjoining surfaces are divided into several parts at the vertices of the adjoining surfaces to be suitable for mesh generation as shown in Fig. 3.

3. Mesh Generation on Trimmed NURBS Surfaces

3.1 Mesh generation on planes

For the mesh generation with quadrilateral elements, a domain decomposition algorithm combined with loop operators is employed, in which the local mesh densities are assigned by the user around the boundaries of the analysis domain (Owen et al., 1998). The analysis domain is transformed into one or several continuous loops by using cut lines and the loops are recursively subdivided into subloops with the use of the best split lines as shown in Fig. 4. Every starting loop must contain an even number of nodes in order to form a quadrilateral mesh.

Among the candidate split lines that connect any two visible nodes in a loop and represent a possible location where the loop could be subdivided, the best split line is determined as in Eq. (3), that is, by minimizing , a linear combination of four dimensionless parameters involving angles(α), areas(β), lengths(γ), and node placement errors(ε).

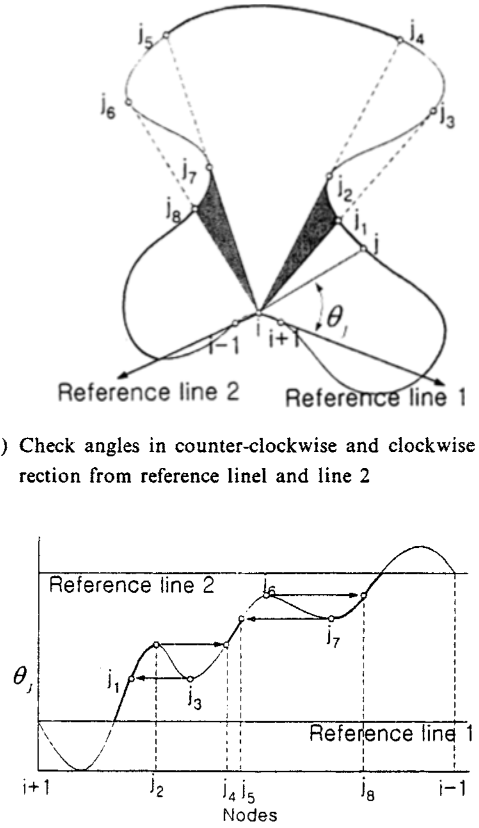

(a) Check angles in counter-clockwise and clockwise direction from reference linel and line 2

(b) A plot of θ_i

Fig. 5 Determination of visible nodes (Talbert, 1991)

$$\text{Minimize } \pi = C_1\alpha + C_2\beta + C_3\gamma + C_4\varepsilon \quad (3)$$

where C_1, C_2, C_3, C_4 are empirically determined constants (Chae et al., 1993).

In order to determine the visible nodes, Talbert and Parkinson (1991) only considered the reference angle as the criterion whether it increases in value from a reference line as shown in Fig. 5. According to this scheme, the nodes from j1 to j2 and from j7 to j8 are considered as invisible from node i, although they are visible. This algorithm is a conservative approximation of the total number of visible nodes from node i in that it will normally eliminate a few more nodes than necessary. However these few eliminated nodes can be

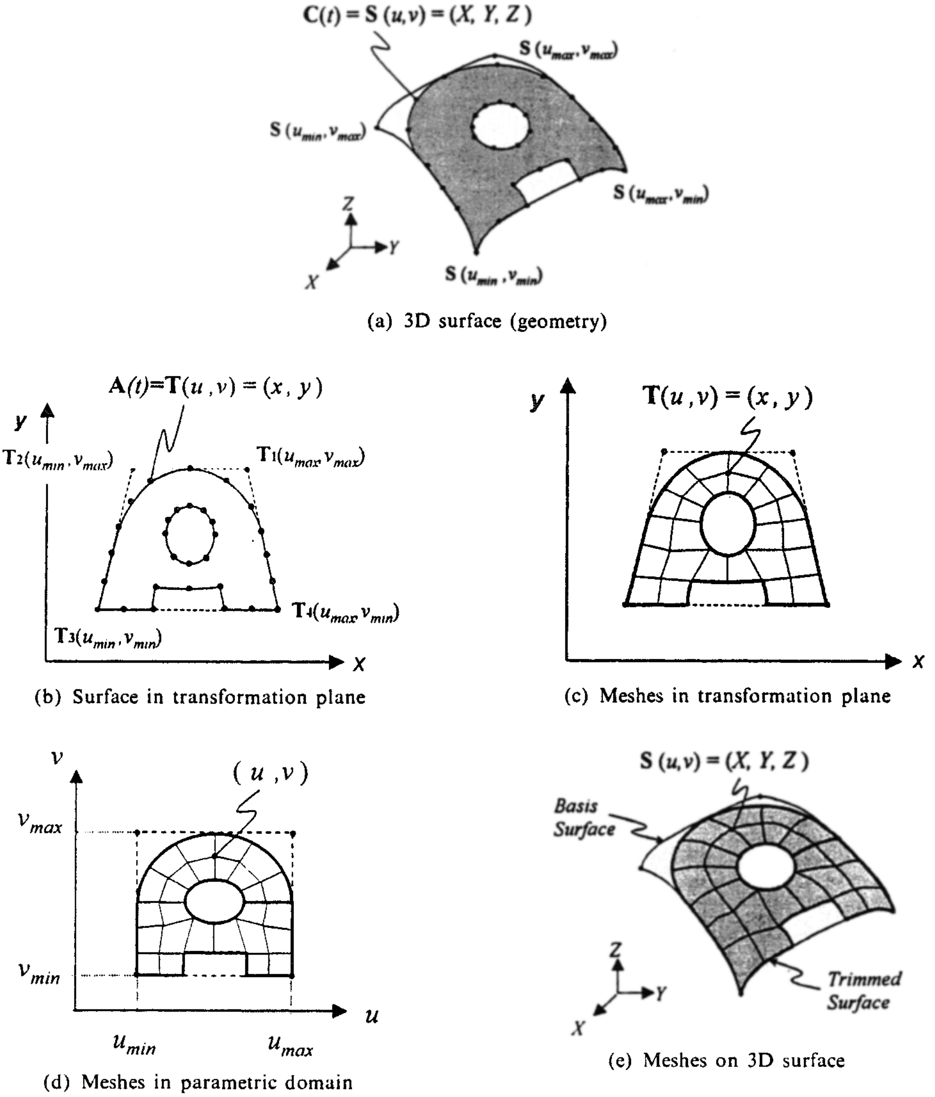

(a) 3D surface (geometry)

(b) Surface in transformation plane

(c) Meshes in transformation plane

(d) Meshes in parametric domain

(e) Meshes on 3D surface

Fig. 6 Mesh generation on trimmed surfaces

critical for the final mesh quality in certain cases. Therefore in this paper a modified criterion has been proposed, which employs both the reference angle and reference distance from a node i. From a given concave boundary node i, visible nodes are examined in the counterclockwise direction from a reference line 1. If an angle θj is larger than the reference angle θ, node j is a candidate visible node. Then the reference angle θ is updated as θj. But, if an angle θj is smaller than the reference angle θ and the following node angle is decreasing, then node j is an invisible node. Finally if an angle θj is smaller than the reference angle θ and the following node angle is increasing, then node θj is a candidate visible node providing that reference distance is increasing. The second pass starts with reference line 2 and goes in the reverse order to reference line 1. Finally two groups of candidate visible nodes are compared to each other. The visible nodes from node i are defined to be only those nodes that are contained in both groups. They are from reference line 1 to node j2 and from j4 to j5 and from j7 to reference line 2. Consequently the visible nodes from j1 to j2 and from j7 to j8 are added to the existing visible nodes obtained by Talbert's scheme.

Using the best split lines, the original boundaries are split recursively until all subloops become six-node loops or eight-node loops, and the corresponding operators complete the mesh generation in each subloop (Chae et al., 1993).

3.2 Mesh generation on surfaces

The proposed mesh generation scheme for three-dimensional surfaces consists of the following steps as shown in Fig. 6.

(1) Determine the types of transformation planes between quasi-expanded planes and projection planes.

(2) Generate key nodes on the boundaries on transformation planes.

(3) Generate quadrilateral meshes on transformation planes.

(4) Transform the meshes to parametric domains.

(5) Transform the meshes in parametric domains to three-dimensional surfaces.

In order to transform the constructed mesh onto the original NURBS surfaces, transformation planes are transformed to u-v parametric planes of the basis surfaces. Then the parametric values (u, v) corresponding to the projection coordinates (x, y) of the generated nodes can be obtained by solving Eq. (4) explicitly.

$$\begin{aligned} T(u, v) &= (x(u, v), y(u, v)) \\ &= (u-u_{\min})(v-v_{\min})T_1 \\ &\quad +(u_{\max}-u)(v-v_{\min})T_2 \\ &\quad +(u_{\max}-u)(v_{\max}-v)T_3 \\ &\quad +(u-u_{\min})(v_{\max}-v)T_4 \qquad (4) \end{aligned}$$

3.2.1 Mesh generation on trimmed NURBS surfaces

As for mesh generation on 3D NURBS surfaces, an indirect 2D approach is employed in this paper, in which both quasi-expanded planes and projection planes are used for 2D transformation planes. Previous work using remapping planes (Lee et al., 1998) may produce distorted elements or fail to construct 2D meshing planes when applied to the surfaces that have severe curvatures inside. On the contrary, the one using projection planes (Chae et al., 1997) may produce more stable meshes than the one using remapping planes in certain types of surfaces with severe curvatures. However, remapping planes may approximate the original surfaces more accurately than projection planes in 2D planes. Therefore in this paper both quasi-expanded planes, an enhancement to the remapping planes, and projection planes are employed for mesh generation. In order to reduce mesh distortion during the back transformation to 3D surfaces as much as possible, quasi-expanded planes are considered at first, and if this planes do not satisfy certain conditions, then projection planes are considered next.

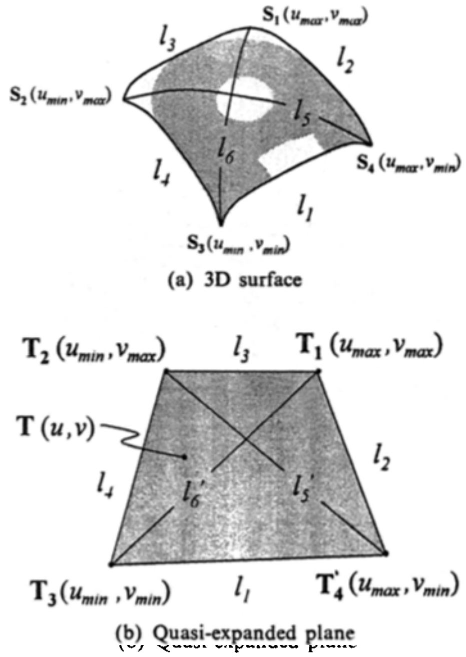

(a) 3D surface

(b) Quasi-expanded plane

Fig. 7 Definition of a quasi-expanded plane

3.2.1.1 Quasi-expanded planes

Quasi-expanded planes are determined by the lengths of the boundary curves and the diagonal curves of basis surfaces. Since this plane also approximates the original surfaces in 2D plane, meshes are constructed on this plane for most of

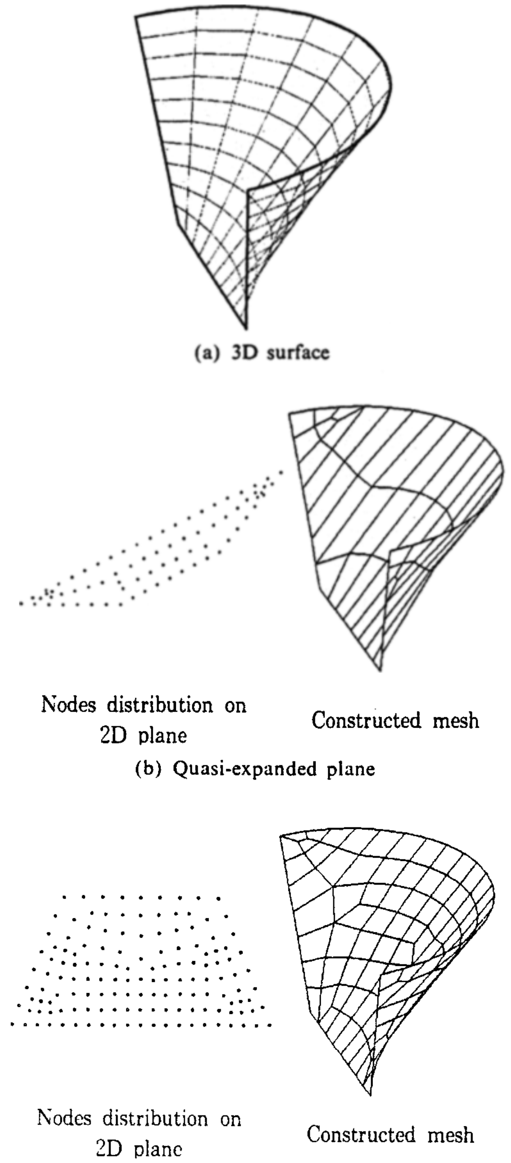

(a) 3D surface

Nodes distribution on 2D plane
Constructed mesh

(b) Quasi-expanded plane

Nodes distribution on 2D plane
Constructed mesh

(c) Projection plane

Fig. 8 2D transformation planes

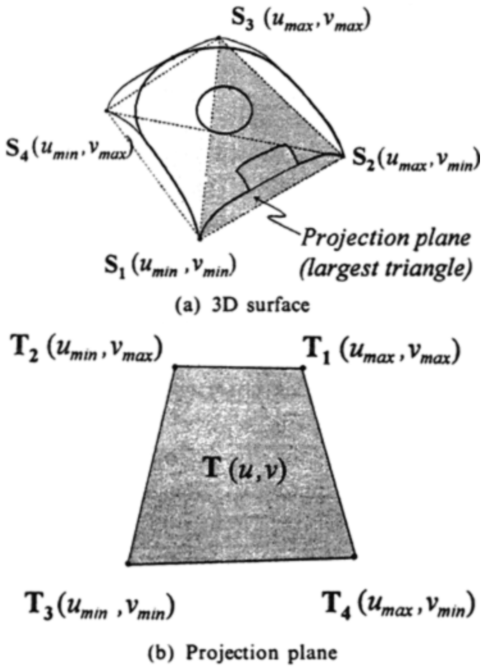

(a) 3D surface

(b) Projection plane

Fig. 9 Definition of a projection plane

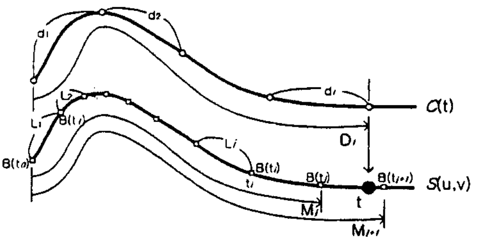

Fig. 10 Placement of boundary nodes

the surfaces. To begin with, the lengths l_1, l_2, l_3, l_4 of four boundary curves and the lengths of two diagonal curves on the basis surfaces are calculated as shown in Fig. 7. Diagonal curves l_5, l_6 are obtained as shown in Fig. 7. With these six lengths, four vertices T_1, T_2, T_3 and T_4 of a quasi-expanded plane are determined. $T_1(x_1, y_1)$ is usually set as the origin for convenience. $T_2(x_2, y_2)$ is determined by using the length l_1. $T_3(x_3, y_3)$ and $T_4(x_4, y_4)$ are determined to satisfy the lengths of l_2, l_3, l_4 and to maintain the ratio of two diagonals, l_5/l_6.

But if the surfaces have severe curvatures, some boundary curves can be much larger than the other curves as shown in Fig. 8(a), which results in the distortions of meshes during the back transformation to 3D surfaces. In addition, if the length of one boundary curve is greater than the lengths of the other three curves, then the transformation plane can not be constructed. Therefore, in our proposed scheme, the condition that the length of each diagonal should be smaller than the sum of the lengths of two opposite boundary curves is employed. Otherwise the following projection planes are used instead.

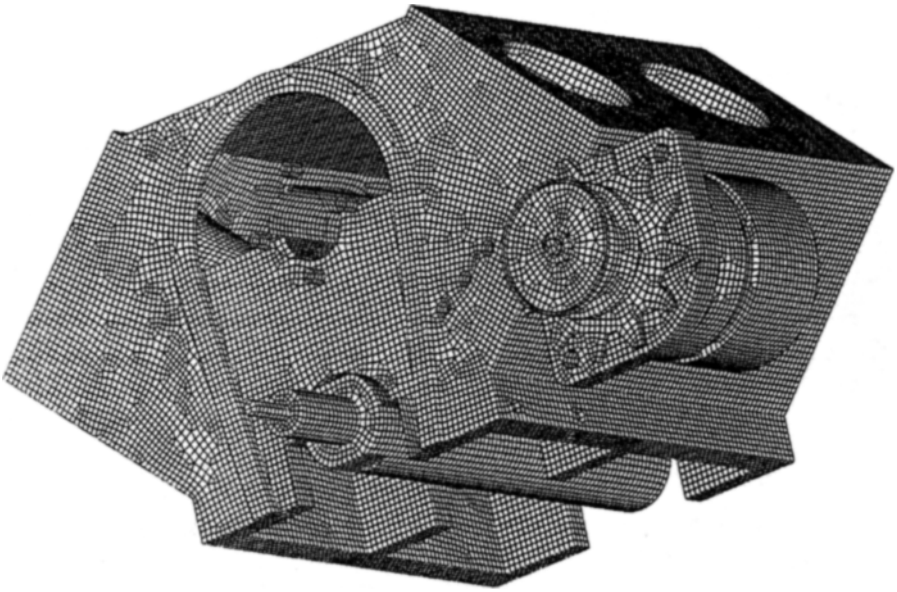

Fig. 11 An engine block model (67941 elements)

3.2.1.2 Projection planes

Once quasi-expanded planes do not satisfy certain conditions, projection planes are considered next. Projection planes are determined by four vertices of a basis surface. This plane is employed for mesh generation on surfaces with singular points such as spherical and conical surfaces. However, the quality of meshes constructed on surfaces with large angle of revolution in the surface of revolution may not be good.

In order to transform a basis surface with four vertices to a projection plane, the plane with the largest projected area is used. For example, four triangles can be constructed from four vertices of a basis surface, and the plane that includes a triangle with the largest area is employed for projection as shown in Fig. 9. Four vertices of a basis surface are projected to this plane, and the quadrilateral area composed of four projected vertices is called a projection plane. Meshes are then constructed in this projection plane.

3.2.2 Boundary node generation

Generally a NURBS curve $C(t)$ is not parametrized uniformly in terms of the parameter t. Therefore, uniformly spaced parameters, t's, of a NURBS curve do not produce uniform spacing of nodes in actual coordinates. In this paper nodes on the boundary curves are generated by considering the distances between nodes. Assume that an equal spacing of nodes is to be generated on a boundary curve. The ith element size and node coordinates are computed as follows.

The size of the ith element is

$$d_i=\frac{l}{N} \tag{5}$$

d_i : Size of the ith element

l : Length of 3D curve

N : Number of elements

and the size map of the ith element length is

$$D_i=\sum_{k=1}^{i} d_k \tag{6}$$

and the size map of surface boundary is

$$M_i=\sum_{k=1}^{i} L_k \tag{7}$$

$$L_i=\overline{S(B(t_i))S(B(t_{i-1}))}\left(t_i=\frac{i}{n}\right) \tag{8}$$

t_i : Parametric value of curve

n : Number of size map on surface boundary

L_i : Part length on surface boundary

After deciding the part position of the ith node

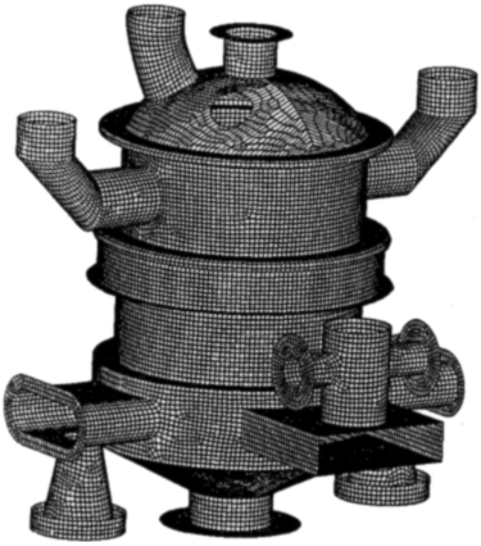

Fig. 12 A pressure vessel model (34488 elements)

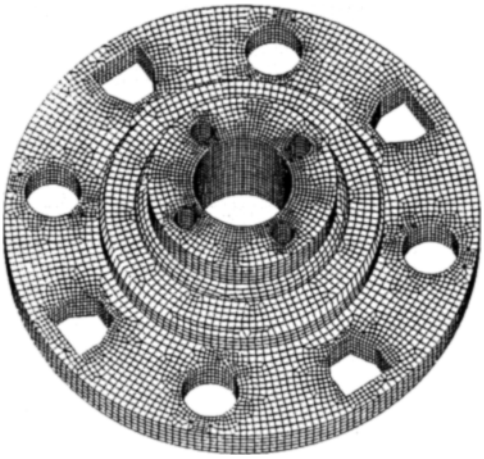

Fig. 13 A wheel model (21767 elements)

using Eq. (9), a new parameter value is calculated by interpolating the length ratio as shown in Fig. 10.

$$M_j < D_i < M_{j+1} \qquad (9)$$

4. Examples

Several examples for the mesh generation are given. Figure 11 shows an example of an engine block model, in which 207 trimmed NURBS surfaces are employed for the mesh generation, resulting in 67941 quadrilateral elements. As shown in Fig. 11, reasonably good meshes are constructed. Another example of a pressure vessel structure is shown in Fig. 12. In this example 86 trimmed NURBS surfaces are employed for mesh generation and 34488 elements are constructed. Figure 13 shows an example of a wheel model, in which 78 trimmed NURBS surfaces are employed and 21767 elements are generated. As shown in Fig. 13, relatively small elements are constructed around holes without severe distortions of elements. As shown in these examples, unstructured quadrilateral meshes are well constructed without any severe distortion of elements.

5. Concluding Remarks

An automatic mesh generation scheme with quadrilateral elements on trimmed NURBS surfaces has been developed. With this scheme reasonably good meshes with different sizes of elements at different locations can be constructed automatically, and the user only needs to define the geometry of a model in the IGES format from an external CAD system. As for the quadrilateral mesh generation, a domain decomposition algorithm has been modified by changing the method of determining the best splitting lines in order to improve the mesh quality. As for the surface meshing, both quasi-expanded planes and projection planes are employed in an indirect 2D approach, which produce better quality of meshes in most of the cases.

6. References

Blacker, T.D. and Stephenson, M.B., 1991, "Paving: A New Approach to Automated Quadrilateral Mesh Generation," *Int. J.Num. Meth. Eng.*, Vol. 32, pp. 811~847.

Cass, R.J., Benzley, S.E., Meyers, R.J. and Blacker, T. D., 1996, "Generalized 3-D Paving: An Automated Quadrilateral Surface Mesh Generation Algorithm," *International Journal for Numerical Methods in Engineering*, Vol. 39, pp. 1475~1489.

Chae, S.W., Shin, B.S. and Min, J.K., 1993, "On the Automatic Mesh Generation with Quadrilateral Finite Elements," *Transactions of the KSME*, Vol, 17, No. 12, pp. 2995~3006.

Chae, S.W. and Jung, J.H., 1997, "Unstructured Surface Meshing Using Operators," *Proc. of the 6th International Meshing Roundtable*, Park City, Utah, October, pp. 281~291.

Farouki, R.T., 1997, "Optimal Paramaterizations," *Computer Aided Geometric Design*, Vol. 14, pp. 153~168.

George, P.L. and Borouchaki, H., 1998, "Delaunay Triangulation and Meshing," *Application to Finite Elements, Hermes, France*, p. 413.

Johnston, B.P., Sullivan, J.M. and Kwasnik, A., 1991, "Automatic Conversion of Triangular Finite Element Meshes to Quadrilateral Elements," *Int. J. Num. Meth. Eng.*, Vol. 31, pp. 67~84.

Lee, C.K. and Lo, S.H., 1994, "A New Scheme for the Generation of a Graded Quadrilateral Mesh," *Comp. Struct.*, Vol. 52, pp. 847-857.

Lee, M.C. and Joun, M.S., "General Approach to Automatic Generation of Quadrilaterals on Three-Dimensional Surfaces," *Commun. Numer. Meth. Engng.*, Vol. 14, pp. 609~620.

Lau, T.S. and Lo, S.H., 1996, "Finite Element Mesh Generation Over Analytical Surfaces," *Computers and Structures*, Vol. 59, No. 2, pp. 301~309.

Lau, T.S. and Lo, S.H. and Lee, C.K., 1997, "Generation of Quadrilateral Mesh over Analytical Curved Surfaces," *Finite Elements in Analysis and Design*, Vol. 27, pp. 251~272.

Owen, S.J, 1998, "A Survey of Unstructured Mesh Generation Technology," *Proc. of 7th International Meshing Roundtable*, Dearbon, Michigan, October, pp. 239~267.

Owen, S.J., Staten, M.L., Canann, S.A. and Saigal, S., 1998, "Advancing Front Quad Meshing Using Local Triangle Transformations," *Proc. 7th International Meshing Roundtable*, Dearborn, Michigan, October, pp. 409~428.

Talbert, J.A. and Parkinson, A.R., 1991, "Development of an Automatic, Two Dimensional Finite Element Mesh Generator using Quadrilateral Elements and Bezier Curve Boundary Definitions," *Int. J. Num. Meth. Eng.*, Vol. 29, pp. 1551~1567.

Tristano, J.R., Owen, S.J. and Cannon, S.A., 1998, "Advancing Front Surface Mesh Generation in Parametric Space Using a Riemannian Surface Definition," *Proc. of the 7th International Meshing Roundtable*, Dearbon, Michigan, October, pp. 429~445.

White, D. R. and Kinney, P., 1997, "Redesign of the Paving Algorithms: Robustness Enhancements Through Element by Element Meshing," *Proc. of the 6th International Meshing Roundtable*, Park City, Utah, October, pp. 323~335.

Zhu, J.Z., Zienkiewicz, O.C., Hinton, E. and Wu, J., 1991, "A New Approach to the Development of Automatic Quadrilateral Mesh Generation," *Int. J. Num. Meth. Eng.*, Vol. 32, pp. 849~866.